TYPE Original Research
PUBLISHED 08 December 2023
DOI 10.3389/fmars.2023.1322899

OPEN ACCESS

EDITED BY
Juan Jose Munoz-Perez,
University of Cádiz, Spain

REVIEWED BY
Lin Zeng,
Ludong University, China
Shenliang Chen,
East China Normal University, China
Wang Qing,
Coastal Research Institute of LuDong University (CRILD), China

*CORRESPONDENCE
Min Xu
xumin0895@njnu.edu.cn

RECEIVED 17 October 2023
ACCEPTED 23 November 2023
PUBLISHED 08 December 2023

CITATION
Li Y, Zhao Y, Xu W, Liu N and Xu M (2023) Quantitative provenance study of sediments in the coastal tidal flats of central Jiangsu based on grain-size End-Member analysis.
Front. Mar. Sci. 10:1322899.
doi: 10.3389/fmars.2023.1322899

Quantitative provenance study of sediments in the coastal tidal flats of central Jiangsu based on grain-size End-Member analysis

Yanxia Li[1,2], Yifei Zhao[1,2], Wenjian Xu[1,2], Nian Liu[1,2] and Min Xu[1,2]*

[1]College of Marine Science and Engineering, Nanjing Normal University, Nanjing, China, [2]Coastal Zone Resources and Environment Engineering Research Center of Jiangsu Province, Nanjing Normal University, Nanjing, China

The coastal mudflats in central Jiangsu Province are influenced by the sediment supply from the Yangtze River and the abandoned Yellow River. However, the sources of sediment in this area have yet to be confirmed, and quantitative studies have been limited. In this study, we addressed this gap by obtaining sediment core samples with lengths of approximately 100 cm from Dongtai and Sheyang, respectively, on the central coast of Jiangsu Province in 2018. The sediment sources were identified and quantitatively evaluated using a grain-size end-member(EM) model. The findings revealed that (1) Sheyang was decomposed into five EMs, with EMs 1-3 originating from the abandoned Yellow River, EM 4 originating from the Yangtze River and the North Jiangsu radial sand ridges (NJRSR), and EM 5 originating from the NJRSR. Over a century scale, the abandoned Yellow River contributed 73.91% to sediment deposition in Sheyang, while the Yangtze River and the NJRSR contributed 26.09%. (2) Dongtai was decomposed into six EMs, with EMs 1-4 originating from the abandoned Yellow River, EM 5 originating from the Yangtze River, and EM 6 originating from the Yangtze River and the NJRSR. Over a century scale, the abandoned Yellow River contributed 70.55% to sediment deposition in Dongtai, and the Yangtze River and the NJRSR contributed 29.45%. (3) On a temporal scale, the contribution of the abandoned Yellow River to sediment deposition on the central mudflats of Jiangsu Province showed an increasing trend. Spatially, the contribution of the abandoned Yellow River to sediment deposition decreased from north to south. (4) There were significant changes in the sediment sources of Sheyang and Dongtai at the depths of 56 cm and 60 cm, respectively, which both experiencing an increased sediment supply from the abandoned Yellow River. In Dongtai, the sediment on the southern side had increased contributions from the abandoned Yellow River due to a reduction in the sediment supply from the Yangtze River. In Sheyang, the sediment on the northern side had increased contributions from the abandoned Yellow River due to the introduction of *Spartina alterniflora*, despite no actual changes in the sediment sources.

KEYWORDS

tidal flats, grain-size, sediment provenance, end-member analysis, central Jiangsu

1 Introduction

Tidal flats, as the most typical area of land-sea interaction, are widely common in the coastal zone and play a vital role in protecting the coastline, supporting high biodiversity, and acting as a barrier against natural disasters, such as storm surges (Barbier et al., 2011; Murray et al., 2014; Zhao et al., 2020a). The formation and evolution of tidal flats are closely related to terrestrial sediment inputs, global climate, and changes in marine dynamic environments (Xu et al., 2014; De Winter and Ruessink, 2017; Zhao et al., 2020b). Despite their significance, tidal flats are currently facing several threats, such as inadequate sediment supply, sea level rise, and human engineering activities, which could potentially result in erosion and degradation (Murray et al., 2014).

The Jiangsu coast is the most typical muddy coastal area in China. The influence of the East China Sea advancing tide wave and the South Yellow Sea rotating tide wave, along with the rich sediment supply from the ancient Yellow River and Yangtze River, has led to the development of the largest and most widely distributed tidal flats in China (Yu et al., 2017; Li et al., 2022) and the North Jiangsu radial sand ridges (NJRSR) (Xu et al., 2019). The mudflats along the central coast of Jiangsu are rich in biodiversity and ecosystem functions. These tidal flat areas serve as crucial habitats for numerous rare and endangered bird species, fish, and shellfish and play a significant role as key stopover sites for migratory birds. The tidal wetlands also serve important functions in protecting the coastline, mitigating storm surges, adsorbing pollutants, and maintaining water quality. However, the muddy coastal areas of central Jiangsu also face several challenges. With the return of the Yellow River to the north and the continuous southward movement of the Yangtze River estuary since 1855, the sediment influx has decreased substantially, leading to varying degrees of erosion in some of the tidal flats (Wang et al., 2006). Insufficient sediment supply, sea-level rise, and human engineering activities are factors that may also have led to the erosion and degradation of the tidal flats, which pose a threat to the tidal flat ecosystems. Therefore, research and conservation efforts are important in this region. Researchers have posited that the material origin of the modern tidal flats off the coast of Jiangsu is jointly controlled by the Yangtze and Yellow rivers (Li and Zhao, 1995; Zhang et al., 2012). Moreover, Zhang (Zhang, 1990) suggested that the material provenance of the northern part of the Jiangsu coast is dominated by the abandoned Yellow River sediments, while the southern part is dominated by the Yangtze River material. Other researchers contend that the present-day coastal sediment along the central coast of Jiangsu is mainly derived from the eroded material of the abandoned Yellow River Delta and the NJRSR, but the relative importance of these two provenances remains unclear (Zhang et al., 2014; Gao et al., 2016).

Furthermore, selecting qualitative indicators and methods to consider the NJRSR in Jiangsu as an independent source is challenging because the sediments of the NJRSR primarily originate from the ancient Yangtze River entering the sea during the Late Pleistocene (Fu and Zhu, 1986). Prior sediment provenance studies of the tidal flats along the Jiangsu coast have mostly used qualitative or semi-quantitative methods and surface samples, and there is a lack of quantitative studies on the contribution rates of the Yangtze River, abandoned Yellow River, and NJRSR over time. Understanding the evolutionary history of the sediment provenance and quantitatively analyzing the contribution rates of these three provenances is of great significance for understanding the characteristics, formation process, and future evolution trends of the sedimentary system of the tidal flats along the coast of Jiangsu.

Recently, with the advancements in modern testing and the development of analytical techniques, especially in mineralogy (Yang et al., 2009), geochemical elemental analysis (Rao et al., 2015), and isotope dating techniques (Dou et al., 2012), the number of provenance analysis methods has increased. However, isotope geochemical methods have high experimental costs and are complex, mineralogical methods are affected by hydrodynamics and diagenesis, and geochemical element methods are affected by grain size.

Sediment grain-size characterization is one of the important indicators of sedimentological characteristics (Lu and An, 1998; Sun et al., 2001; Li et al., 2010; Wang et al., 2021), and its use in exploring the depositional provenance and environment has become a hot topic in sedimentology (Sahu, 1964; Visher, 1969; Folk, 1971; Gao et al., 1994; Purkait, 2010). When compared with the traditional grain-size analysis method, grain-size EM analysis can more effectively utilize high-precision grain-size data, effectively decompose the sediment grain-size data into multiple EMs of different provenances, and further reveal the provenance and sedimentary dynamics (Sun et al., 2003; Zhu et al., 2020). However, most of the previous studies have been limited to the analysis of the transport range and influencing factors of marine surface sediments (Zhang et al., 2006; Xue et al., 2018), and there has been no systematic analysis of the changes in sediment provenance in the same sediment body over time. This study aimed to fill the research gap in understanding the temporal variations in sediment sources within the same depositional system using sediment grain size analysis. By employing an EM-based approach, this study investigated the sources and changes in sediment in the Jiangsu coastal tidal flats over a century-scale, and the sedimentary environmental information that was inferred from these changes was examined. The study quantitatively examined the contributions of the abandoned Yellow River, the Yangtze River, and the NJRSR to the sediment composition in the central Jiangsu tidal flats. The objective was to provide scientific references for the future development and utilization of the Jiangsu coastal tidal flats. Additionally, this study sheds light on the evolutionary processes, sediment dynamics, and the impacts of changes in the sediment sources on the depositional environment of the Jiangsu coastal tidal flats. This knowledge holds significant importance for future coastal tidal flat management, coastal engineering planning, and ecological conservation.

2 Materials and methods

2.1 Study area

The central coast of Jiangsu Province spans several hundred kilometers, encompassing cities such as Lianyungang, Yancheng, and Nantong. The coastal region exhibits diverse and complex geomorphology, including bays, estuaries, sandbars, tidal flats, and islands. Along the coast, there are a series of natural tidal flats and estuarine wetlands, such as the *Spartina alterniflora* marshes. The stems and leaves of *Spartina alterniflora* have a strong buffering effect on the water flow, which significantly reduces the velocity and sediment transport capacity, thus, capturing suspended sediment (Xu et al., 2009). The coastal area is influenced by several modern oceanic current systems, including the Shandong Coastal Current (SDCC), Yellow Sea Coastal Current (YSCC), diluted water from the Yangtze River (CDW), and the warm current of the Yellow Sea (YSWC). These currents contribute to the region's strong tidal action and large tidal range (Meng, 2018). The area belongs to a subtropical monsoon climate, and it is significantly affected by extreme weather events such as storm surges throughout the year (Yang, 2017). Additionally, the central coast of Jiangsu possesses rich ecological resources, including coastal wetlands and bird habitats. These ecosystems play a vital role in maintaining the ecological balance of the coastal zone and protecting endangered species. Therefore, the central coast of Jiangsu is a geographically significant coastal region with diverse landforms and significant influences from the ocean and climate. It has abundant ecological resources and is affected by human economic activities, making it crucial for sustainable development and ecological conservation in the region.

2.2 Collection samples

Two cylindrical (core) samples (Sheyang [SY] and Dongtai [DT]) with lengths of 106 cm and 100 cm, respectively, were drilled from north to south using a portable gravity sampler on the tidal flats of the central muddy coast of Jiangsu during July–August 2018. The sampling locations are shown in Figure 1. The samples were sealed, refrigerated at a low temperature, and transported back to the laboratory, where the SY and DT core samples were divided into 2 cm-vertical pieces. The sampling tool was thoroughly cleaned with deionized water between each division to avoid contaminating the adjacent samples.

2.3 Sample testing methods

2.3.1 Grain size of the sediment samples

Before the grain-size analysis, 15–20 mL of 30% H_2O_2 solution was added to remove the organic matter, and the samples were immersed in 10% HCl solution (10 mL) for 48 h to remove the calcium carbonate. The sediment grain size was then determined using a laser grain-size analyzer (the Mastersizer 2000 laser grain-size analyzer; Malvern Company, United Kingdom). The operation steps included weighing ~2.5 g (depending on the size of the sample particles) of the sediment sample in a 100 mL beaker with 20 mL sodium hexametaphosphate solution (0.5 mol/L) and stirring it well. The sodium hexametaphosphate solution was continually added to fill up the beaker, which was left to stand for 24 h before loading. The measurement range of the analyzer was 0.01–1000 μm, and the grain-size resolution was 0.01 μm. The relative error of the repeated measurements was less than 3%. The experiments were conducted at the Key Laboratory of the School of Marine Science and Engineering at Nanjing Normal University, China.

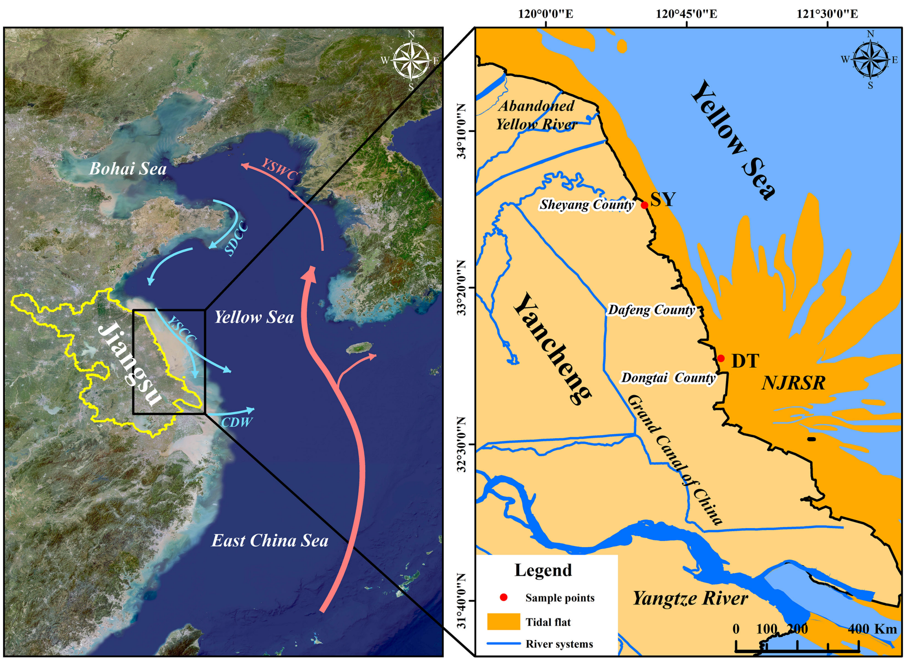

FIGURE 1
Schematic map of the study area, including Dongtai (DT), Sheyang (SY), and the north Jiangsu radial sand ridges (NJRSR). The modern current systems within the study area are shown: Shandong Coastal Current (SDCC), Yellow Sea Coastal Current (YSCC), Changjiang Diluted Water (CDW), and the Yellow Sea Warm Current (YSWC).

2.3.2 Radionuclide dating

The sediment radioactivity of ^{210}Pb and ^{137}Cs were measured using γ analytical methods. After collection, the samples were quickly dried, weighed, ground, put into test tubes, and sealed with wax. The GEM high-purity germanium detector, DSPEC-jr series digital spectrometer, and multi-channel analysis system (ORTEC) were used for the analysis. The excess ratio activity of ^{210}Pb was obtained by subtracting the background value of ^{210}Pb in the sediment from the measurement of ^{226}Ra. The sample analysis was completed at the Institute of Geography and Lakes of the Chinese Academy of Sciences in Nanjing, China.

2.4 Data analysis methods

2.4.1 Grain-size EM analysis

Weltje (Weltje, 1997) proposed the concept of EM components based on the analysis of grain-size data. EM analysis can effectively decompose the sediment grain-size data into many EMs of specific and different provenances (Xue et al., 2018; Liu et al., 2021), aiding in the quantitative identification of the sediment provenance and the transport mechanism. This gives this method a clear advantage in the study of sediment provenance. According to the concept of EM components, the grain-size data X of sediment can be expressed as a combination of multiple EM components B:

$$X = M \cdot B \tag{1}$$

Where X is the sediment grain-size matrix; M is the relative content matrix; B is the EM component matrix; and X , M , and B are all one-dimensional matrices where the sum of the matrix elements is 100%. Since the samples are a mixture of dynamic components with a sum of 100%, the sediment grain-size matrix, relative content matrix, and EM component matrix in Eq. (1) are all compositional data.

Based on the above principle, this study analyzed the grain-size data using the Analysize-Masters software package that was provided by Paterson and Heslop (Paterson and Heslop, 2015) and runs in Matlab. The software includes both parametric and nonparametric methods and contains four types of parametric methods. Li et al. (Li et al., 2018) performed a comprehensive analysis and comparison of the parametric and nonparametric methods and concluded that the results that were obtained using the Weibull analysis option of the parametric methods were more desirable when the sedimentary dynamics were continuous and relatively stable. Given the complex hydrodynamic conditions and provenance characteristics of the central Jiangsu coast and the stability of the sedimentary dynamics and provenances, this study adopted the parametric Weibull distribution function for the analysis.

2.4.2 Sediment age determination

The sediment from the potential sediment sources is the primary contributor to ^{210}Pb deposition. The provenance determines the amount of ^{210}Pb that is deposited, and an increase in sediment leads to an increase in ^{210}Pb. It was calculated using the following formula (Li and Gao, 2012):

$$C_h = C_0 \times e^{-\lambda t} \tag{2}$$

where C_h is the specific activity (Bq/kg) of ^{210}Pb at a mass depth of h in the sediment profile; C_0 is the specific activity (Bq/kg) of ^{210}Pb at a mass depth of 0 ; and λ is the decay coefficient, which is 0.03114a; and t is time.

3 Results and analysis

3.1 Grain-size characteristics of the sediments

The sediment grain-size characteristics typically include the grain size distribution and mean grain size. As shown in Figure 2, both Sheyang and Dongtai were dominated by sand and silt, with a smaller clay content. Dongtai had a higher proportion of silt when compared with that of Sheyang, while Sheyang had a higher sand content. Over time, both regions had an increasing trend in the silt content and a decreasing trend in the sand content. The mean grain size reflected the sediment coarseness (Gao, 2015), which ranged from 8.84 to 60.90 μm in Sheyang, with a mean value of 38.39 μm, and ranged from 12.00 to 53.34 μm in Dongtai, with a mean value of 29.84 μm.

The sand content in both of the core samples varied significantly with depth. As the depth decreased, the silt content in Sheyang (average of 63.20%) and Dongtai (average of 70.75%) showed an increasing trend, indicating that silt was the dominant sediment in the nearshore deposits. The variation in the mean grain size with depth (Figure 2), revealed a significant decreasing trend in the grain-size fluctuation with depth. In particular, at the depths of 60 cm in Dongtai and 56 cm in Sheyang, the variation in the mean grain size was more pronounced. The significant changes in the grain size with depth in the core samples suggest possible variations in the sediment sources.

3.2 Sedimentation rate analysis

Since the Sheyang sampling site was in the *Spartina alterniflora* marsh, the sedimentation rate variation was influenced by *Spartina alterniflora*. According to the profile structure, the sedimentation rate for 65–0 cm was 1.67 cm/a, and the sedimentation rate for 106–65 cm was 0.88 cm/a (Zhao et al., 2021). The depositional age of the Sheyang core samples ranged from 1942 to 2018.

The results of the ^{210}Pb analysis showed that the maximum activity of the whole vertical profile was 155.8 Bq/kg, the minimum activity was 41 Bq/kg, and the average activity was 80.05 Bq/kg. In addition, at approximately 90 cm, the ^{210}Pb activity value was consistent with the activity value of ^{226}Ra and reached the background value. Based on the linear regression analysis, the Dongtai sediment deposition rate was 1.068 cm/a. The ^{137}Cs test results showed that all the activity values were 0; thus, the sediment deposition rate could not be determined. Therefore, the results of the ^{210}Pb activity calculations were used as the average deposition rate in this core sample. Consequently, the sediments were dated from 1918 to 2018 (Figure 3).

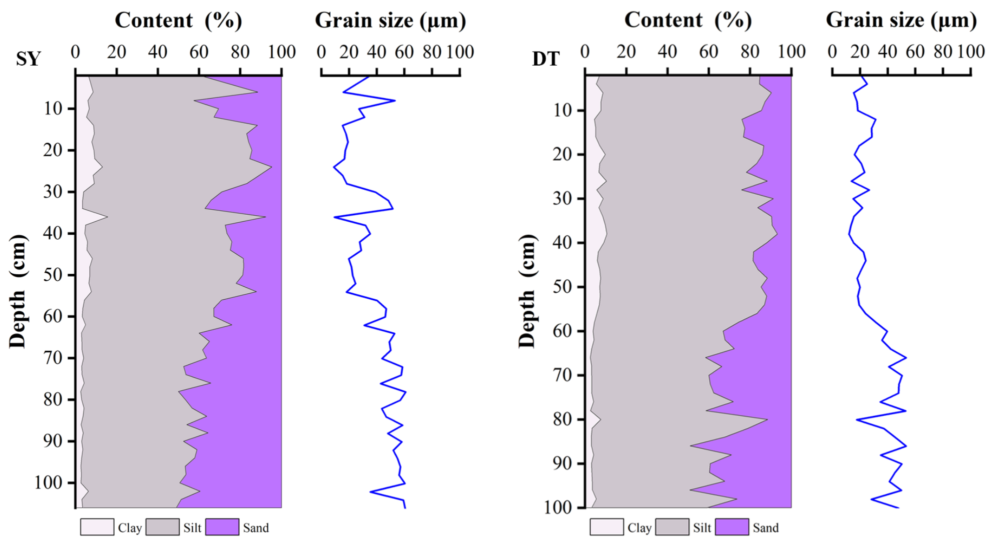

FIGURE 2
Variation in sand-silt-clay content of SY and DT cores and Variation in average grain size of SY and DT cores.

3.3 Sediment grain-size EM determination

When performing the EM modeling on the 53 samples from the Sheyang borehole and 50 samples from the Dongtai borehole, a smaller EM correlation (EM R^2) was desirable to minimize the number of selected EMs while ensuring an angular deviation of less than five degrees and maximizing the linear correlation coefficient R^2 (Xue et al., 2018). As shown in Figure 4, selecting five EMs for Sheyang was the most reasonable. When the number of Dongtai EMs was 3, the angular deviation was greater than 5; when the number of EMs was 4 or 5, the EM R^2 was greater than that when the number of EMs was 6; and the linear correlation was maximized

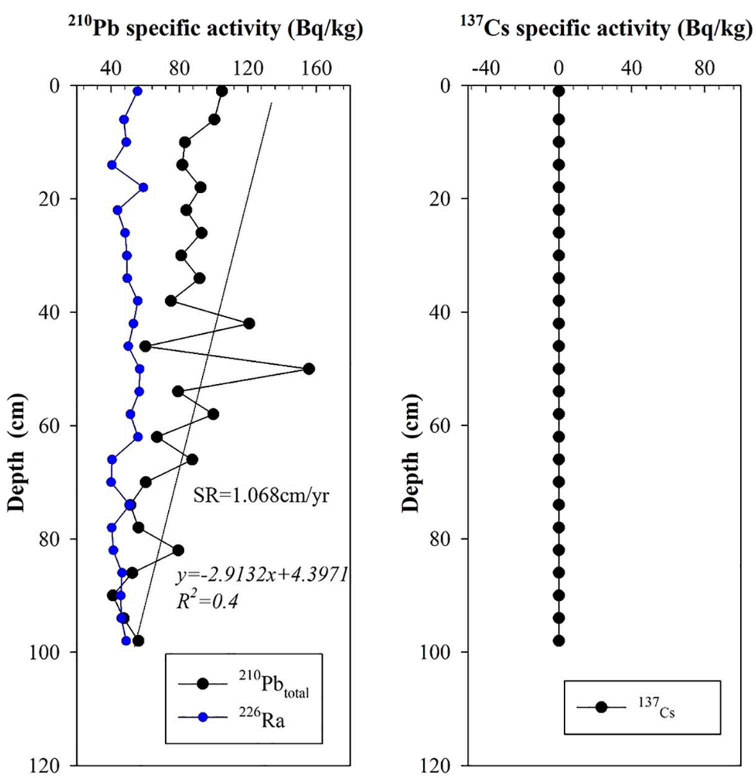

FIGURE 3
Deposition rate of DT.

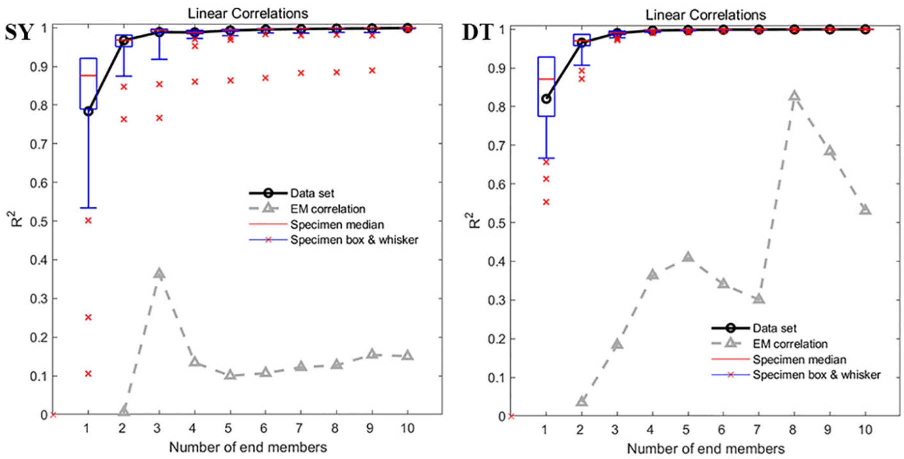

FIGURE 4
Parameterized EM fitting and EM number selection for each Weibull profile.

when the number of EMs was 6. Therefore, six EMs were chosen for the Dongtai analysis. The specific EMs that were obtained for each region can be seen in Table 1. An inverse analysis of the EMs was conducted on the grain-size data of the selected EMs of the various regions. The end-element fit and percentages are shown in Table 2. In terms of the decomposition of the EMs, the grain size of EM increased sequentially, while the clay content gradually decreased, and the sand content increased for each EM (Figure 5). Except for Sheyang EM 5, the sorting coefficient of the remaining regions' EMs gradually decreased, indicating improved sorting. Except for EM 1 and Sheyang EM 5 all the other EMs were negatively skewed.

3.4 Determination of the potential provenance regions for each EM

The sediment grain-size characteristics are one of the most important indicators for understanding sedimentary environments and provenances. In this study, under the assumption of three potential sediment sources (the abandoned Yellow River, Yangtze River, and the NJRSR), the analyzed relevant grain-size distribution and mean grain-size of each EM were correlated with the relevant parameters of the provenance areas (Gao, 2015; Yang, 2017; Cao et al., 2021) using SPSS 20. The results of the analyses are shown in Table 3. For Sheyang, Ems 1-3 had strong correlations with the abandoned Yellow River sediments, EM 4 had a strong correlation with the Yangtze River and the NJRSR sediments, and EM 5 had a stronger correlation with the NJRSR sediments than with the other sediments. For Dongtai, EMs 2-4 had a strong correlation with the abandoned Yellow River sediments, EM 5 had a strong correlation with the Yangtze River sediments, and EM 6 had a stronger correlation with the Yangtze River and the NJRSR sediments than with the abandoned Yellow River sediments. However, the correlation between Dongtai EM 1 and the potential source regions was not determined.

Further exploration of the relationships between each EM and the potential sediment sources was conducted based on a comparison between the correlation data of each EM of the two core samples from Sheyang and Dongtai and the sand-silt-clay content of the potential sediment source (Figure 6A). It was found that the data related to Dongtai EM 1 were closer to those of the abandoned Yellow River, while the potential source regions and correlation analysis of the other EMs yielded similar results. The sand content of each EM and potential sediment source varied the most (Figure 2), and the average grain size of the potential sediment sources and each EM varied significantly, which could indicate sediments from different provenances. Therefore, the ratio of the average grain size to the sand content was used as a correlation index to determine the potential sediment source (Figure 6B). The results were consistent with the results that were obtained from the two methods that were mentioned above, further indicating the correlation between Dongtai EM 1 and the sediment from the abandoned Yellow River. Therefore, the sediments in this area mainly originated from the abandoned Yellow River. However, none of the above methods could accurately distinguish the EMs from the Yangtze River and the NJRSR, and thus the contribution of the Yangtze River and the NJRSR to the two areas could not be confirmed. This may be because the sediments from the NJRSR were mainly derived from the ancient Yangtze River entering the sea (Fu and Zhu, 1986), and despite the grain-size data for the

TABLE 1 Parameterized EM fitting properties for each region.

Core ID	No. of EMs	R^2	Theta	EM R^2
SY	5	0.9930	4.3715	0.1001
DT	6	0.9989	1.6930	0.3401

TABLE 2 Characteristics of each EM of SY and DT cores.

EM	Mz (microns)	Sigma (microns)	Skewness	Kurtosis	Percentage
SY-EM 1	7.98	3.66	0.02	0.96	32.09
SY-EM 2	30.36	1.34	-0.17	1.00	10.86
SY-EM 3	45.27	1.38	-0.18	1.02	30.96
SY-EM 4	69.41	1.39	-0.18	1.04	23.76
SY-EM 5	232.62	2.54	0.12	0.96	2.33
DT-EM 1	4.02	3.58	0.10	0.96	21.54
DT-EM 2	15.71	2.07	-0.06	0.98	20.31
DT-EM 3	23.98	1.41	-0.14	1.01	6.54
DT-EM 4	36.56	1.47	-0.17	1.02	22.16
DT-EM 5	59.06	1.50	-0.17	1.03	26.71
DT-EM 6	104.85	1.30	-0.18	1.04	2.74

sediments from the NJRSR and Yangtze River being quite different, the particles that were deposited in the *Spartina alterniflora* marsh all had small grain-sizes. Therefore, distinguishing the two according to grain size was difficult.

Sheyang's EMs 1-3 were derived from the abandoned Yellow River, EM 4 was derived from the Yangtze River and the NJRSR, and EM 5 was derived from the NJRSR. Additionally, Dongtai's EMs 1-4 were all derived from the abandoned Yellow River, EM 5 was derived from the Yangtze River, and EM 6 was derived from the Yangtze River and the NJRSR.

On a century scale, the contribution of the abandoned Yellow River to sediment in the Sheyang region was approximately 73.91%, and it was approximately 70.55% in the Dongtai region. The contribution of the Yangtze River and the NJRSR to sediment in the Sheyang region was approximately 26.09%, and it was approximately 29.45% in the Dongtai region. Therefore, on a century scale, the abandoned Yellow River contributed approximately 72.23% of the sediment in the central muddy coast of Jiangsu, while the Yangtze River and the NJRSR contributed approximately 27.77% of the sediment.

4 Discussion

4.1 Primary factors influencing the sediment source changes

Figure 7 shows that over a century scale, the tidal flat sediment on the muddy coast of central Jiangsu Province was primarily derived from the abandoned Yellow River but it also included contributions from the Yangtze River and the NJRSR. This finding was consistent with previous studies (Gao, 2015; Yang, 2017; Cao et al., 2021). Over time, the proportion of sediment from the abandoned Yellow River gradually increased, while contributions from the Yangtze River and the NJRSR decreased. Significant changes in the two sediment sources were noted at a depth of 56

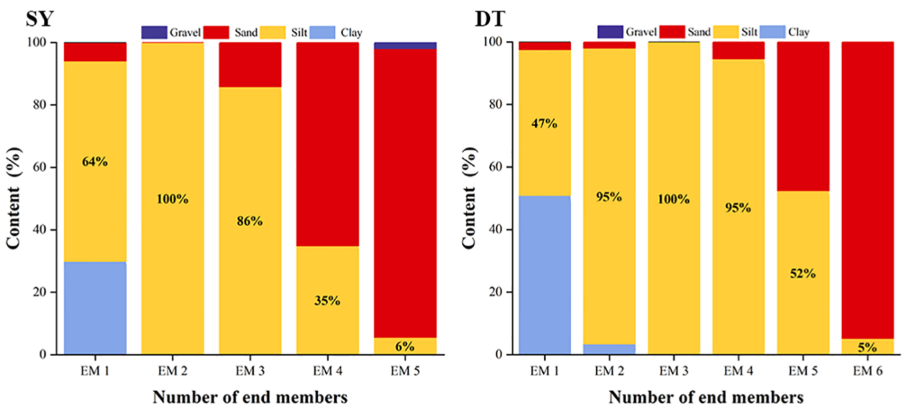

FIGURE 5
Percentage of sand-silt-clay content for each EM of SY and DT cores.

10.3389/fmars.2023.1322899

TABLE 3 Correlation of SY and DT EMs with sediment from the source area(Data from [dataset] [Gao, 2015; Yang, 2017; Cao et al., 2021]).

SY-Pearson correlation - standard format																		
	Mean	standard deviation	1	2	3	4	5	6	7	8	9	10	11	12	13	14	15	16
Abandoned Yellow River(1)	25.842	25.194	1															
Abandoned Yellow River(2)	22.240	33.310	0.870	1														
Abandoned Yellow River(3)	20.910	33.218	0.792	0.988**	1													
Abandoned Yellow River(4)	21.674	29.006	0.769	0.973**	0.994**	1												
Yangtze River(5)	26.942	23.183	0.937*	0.648	0.542	0.519	1											
Yangtze River(6)	28.240	23.660	0.837	0.461	0.341	0.323	0.974**	1										
Yangtze River(7)	32.024	31.564	0.433	-0.064	-0.191	-0.197	0.713	0.854	1									
NJRSR(8)	36.500	37.918	0.395	-0.093	-0.225	-0.227	0.659	0.807	0.975**	1								
NJRSR(9)	37.862	41.584	0.325	-0.165	-0.295	-0.295	0.603	0.763	0.968**	0.997**	1							
NJRSR(10)	35.514	38.316	0.259	-0.240	-0.360	-0.356	0.562	0.734	0.976**	0.982**	0.990**	1						
NJRSR(11)	40.964	49.284	0.233	-0.255	-0.380	-0.377	0.520	0.694	0.945*	0.985**	0.995**	0.988**	1					
EM1	21.598	26.340	0.748	0.954*	0.984**	0.996**	0.504	0.310	-0.199	-0.238	-0.305	-0.356	-0.386	1				
EM2	26.072	43.350	0.914*	0.958*	0.906*	0.878	0.727	0.570	0.086	0.099	0.027	-0.073	-0.057	0.841	1			
EM3	29.054	36.715	0.951*	0.875	0.793	0.767	0.838	0.727	0.315	0.341	0.274	0.172	0.194	0.727	0.968**	1		
EM4	33.882	33.678	0.507	0.023	-0.113	-0.123	0.757	0.883*	0.986**	0.988**	0.976**	0.960**	0.950*	-0.135	0.201	0.432	1	
EM5	66.523	100.706	0.111	-0.294	-0.408	-0.396	0.338	0.506	0.773	0.890*	0.907*	0.867	0.932*	-0.416	-0.060	0.180	0.818	1

*p<0.05, **p<0.01.

DT-Pearson correlation - standard format																			
	Mean	standard deviation	1	2	3	4	5	6	7	8	9	10	11	12	13	14	15	16	17
Abandoned Yellow River(1)	25.842	25.194	1																
Abandoned Yellow River(2)	22.240	33.310	0.870	1															
Abandoned Yellow River(3)	20.910	33.218	0.792	0.988**	1														
Abandoned Yellow River(4)	21.674	29.006	0.769	0.973**	0.994**	1													

(Continued)

TABLE 3 Continued

DT-Pearson correlation - standard format																			
	Mean	standard deviation	1	2	3	4	5	6	7	8	9	10	11	12	13	14	15	16	17
Yangtze River(5)	26.942	23.183	0.937*	0.648	0.542	0.519	1												
Yangtze River(6)	28.240	23.660	0.837	0.461	0.341	0.323	0.974**	1											
Yangtze River(7)	32.024	31.564	0.433	-0.064	-0.191	-0.197	0.713	0.854	1										
NJRSR(8)	36.500	37.918	0.395	-0.093	-0.225	-0.227	0.659	0.807	0.975**	1									
NJRSR(9)	37.862	41.584	0.325	-0.165	-0.295	-0.295	0.603	0.763	0.968**	0.997**	1								
NJRSR(10)	35.514	38.316	0.259	-0.240	-0.360	-0.356	0.562	0.734	0.976**	0.982**	0.990**	1							
NJRSR(11)	40.964	49.284	0.233	-0.255	-0.380	-0.377	0.520	0.694	0.945*	0.985**	0.995**	0.988**	1						
EM1	20.805	25.605	0.346	0.666	0.764	0.821	0.098	-0.071	-0.445	-0.474	-0.514	-0.525	-0.560	1					
EM2	23.142	40.422	0.903*	0.987**	0.952*	0.924*	0.699	0.524	0.011	-0.006	-0.080	-0.166	-0.169	0.542	1				
EM3	24.795	43.300	0.910*	0.971**	0.926*	0.896*	0.716	0.551	0.053	0.054	-0.018	-0.113	-0.105	0.491	0.995**	1			
EM4	27.313	40.550	0.933*	0.934*	0.872	0.844	0.771	0.630	0.169	0.187	0.117	0.015	0.033	0.416	0.972**	0.989**	1		
EM5	31.811	29.325	0.790	0.401	0.266	0.247	0.925*	0.968**	0.863	0.870	0.831	0.778	0.776	-0.170	0.486	0.535	0.637	1	
EM6	40.970	53.896	0.137	-0.357	-0.475	-0.471	0.449	0.639	0.938*	0.962**	0.979**	0.990**	0.991**	-0.609	-0.277	-0.219	-0.086	0.705	1

*p<0.05, **p<0.01.

10.3389/fmars.2023.1322899

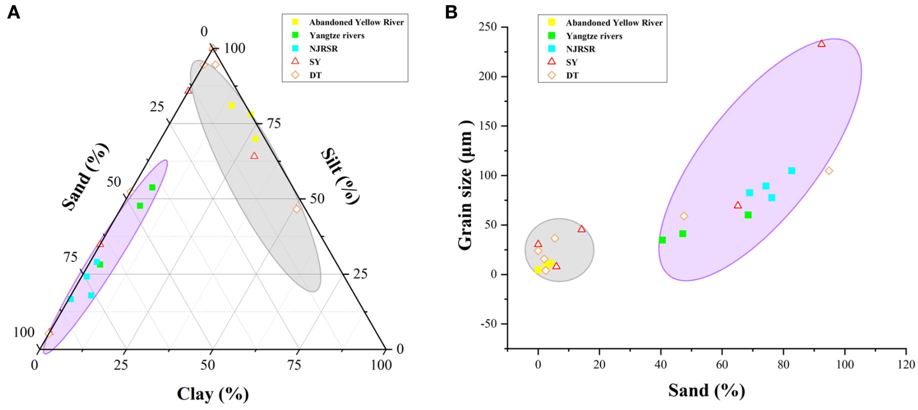

FIGURE 6
(A) Clay-Silt-Sand content diagram of SY, DT, and potential source areas. **(B)** Correlation diagram of sand-average Grain Size of SY, DT, and potential source areas (Data from [dataset] [Gao, 2015; Yang, 2017; Cao et al., 2021)].

cm (1984) for the Sheyang core and 60 cm (1962) for the Dongtai core. The contributions from the Yangtze River and the NJRSR were significantly lower at these depths when compared with those between 106-56 cm and 100-60 cm.

Over the past century, the hydrodynamics of the tidal flats along the coast of central Jiangsu Province have remained relatively stable. However, since 1950, intensified human activities in the Yangtze River Basin, particularly the construction of reservoirs, led to a decreasing trend in sediment discharge from the Yangtze River into the sea (Gao et al., 2018; Liu et al., 2021). The variations in the sediment quantity and source composition of the Yangtze River's input material, which serves as a source for the sediment on the muddy coast of central Jiangsu Province, impact the sediment grain size and composition of the tidal flats (Gao et al., 2019). Consequently, there have been reduced contributions of Yangtze River sediment to the coast of central Jiangsu Province, which has affected the corresponding sediment records. The Dongtai core, which was more influenced by the Yangtze River, had a decrease in Yangtze River-derived sediment and a relative increase in abandoned Yellow River-derived sediment after approximately 1962. This is consistent with the decrease in the sediment discharge from the Yangtze River, indicating that the reduction in Yangtze River sediment was likely the direct cause of the changes in the sediment sources in the tidal flats of central and southern

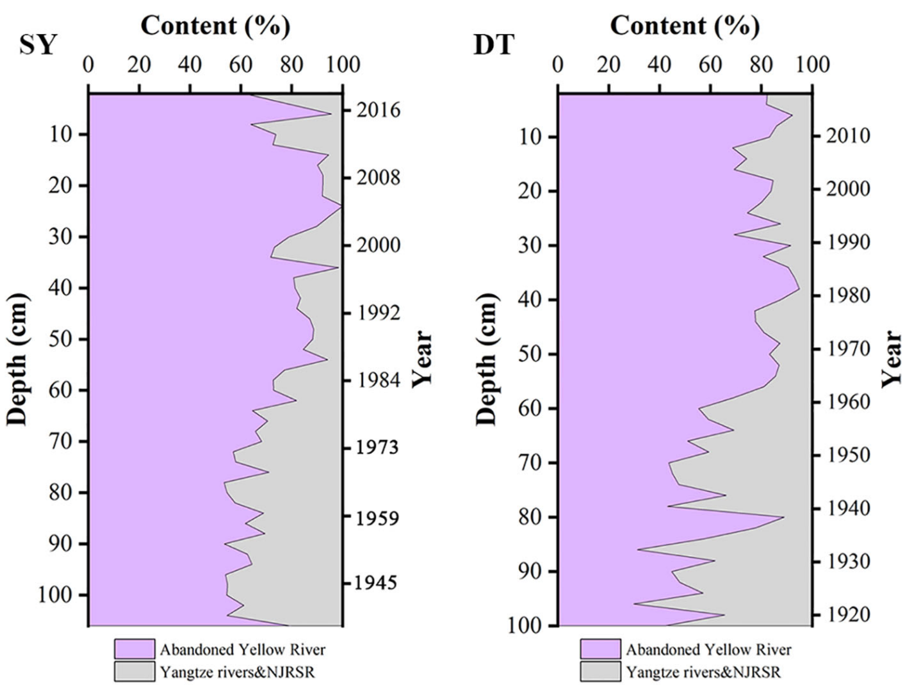

FIGURE 7
Variation in contribution amount from SY, and DT source areas with depth.

Jiangsu Province after 1962. Moreover, despite reduced sediment discharge from the Yangtze River, the abundant sediment supply from the abandoned Yellow River and the NJRSR contributed to the continued accretion of the tidal flats in central and southern Jiangsu Province during this period.

The decrease in the sediment discharge from the Yangtze River around 1962 did not significantly impact the Sheyang core, which was located in the northern part of central Jiangsu Province. This is mainly because the Sheyang core was situated north of the NJRSR, where the Yangtze River sediment supply is limited. However, around 1984, there was a noticeable change in the sediment sources in the northern part of the Sheyang core, which may be linked to the invasion of *Spartina alterniflora*. Introduced into the Sheyang area in the 1980s due to its wave-breaking and sediment-trapping effects, *Spartina alterniflora* created areas of weak current and facilitated fine particle deposition. This led to the formation of sediment with finer grains and a higher clay content without a significant change in the sediment sources. Therefore, the increase in sediment from the abandoned Yellow River that was observed in the Sheyang core around 1984 was not a reflection of a change in the sediment sources but rather because of finer sediment particles due to the accretion that was facilitated by *Spartina alterniflora*.

Another noteworthy issue along the coast of central Jiangsu Province was the ongoing southward migration of the NJRSR and the increasing erosion of the coastal areas, particularly with the decrease in sediment from the Yangtze River, the near depletion of the abandoned Yellow River delta, and the exacerbation of global changes and human activities. However, the central and southern parts of the coastal area in Jiangsu Province still experienced slight accretion. Considering these changes, the future sediment sources for the tidal flats on the muddy coast of central and southern Jiangsu Province may primarily involve alterations in the already existing sediments. Further research is needed to fully determine the applicability of the grain-size EMs method for quantitative analysis of sediment sources on this coast.

4.2 Challenges in distinguishing sediment from the Yangtze River and the NJRSR using grain-size EM analysis

The grain-size EMs analysis method may be unable to distinguish sediment sources, such as the Yangtze River and the NJRSR. The main reasons are as follows.

First, they had similar sediment grain-size characteristics. The sediment from the Yangtze River and the NJRSR had similarities in grain size. This was mainly because the NJRSR initially developed under the influence of a sediment supply from the Yangtze River and the Yellow River, which resulted in similar source characteristics (Fu and Zhu, 1986), such as the rock types and depositional environments. In such cases, relying solely on grain-size EMs analysis may not be sufficient to differentiate between different sediment sources.

Second, they may be difficult to distinguish due to the sedimentary environment and grain size variation. The NJRSR was continuously subjected to marine tidal currents and wave action during its formation and afterward, leading to coarsening of the surface sediments. This coarsening made the grain-size characteristics of the sediment more similar to those of the sediment of the Yangtze River. This made it challenging to quantitatively distinguish between the two sources using grain-size EMs analysis.

Third, the data were incomplete. Grain-size EMs analysis requires a large amount of sample data for accurate interpretation and comparison. The limited number of samples that were obtained in this study would have limited the precise differentiation of the sediment sources (Dietze and Dietze, 2019), such as the Yangtze River and the NJRSR.

To overcome these challenges, a multi-indicator comprehensive analysis should be considered. In addition to the grain-size EMs analysis, combining other geochemical indicators and isotope characteristics could enhance the identification capabilities of the sediment sources. Different sources may exhibit differences in chemical composition and isotopic composition, and comprehensive analysis could improve their differentiation. In conclusion, distinguishing sediment sources, such as the Yangtze River and the NJRSR, requires the comprehensive consideration of multiple methods and factors, and further research is needed to obtain more accurate results.

4.3 Applicability of grain-size EMs analysis in nearshore tidal flat sediment source studies

Grain-size EMs analysis is a method that is used to determine the contributions of different sediment sources in sediments by analyzing the grain-size distribution. In nearshore tidal flat sediment source studies, the grain-size EMs analysis method has some applicability, but several aspects need to be considered.

First, the source characteristics need to be considered. Nearshore tidal flat sediments may be influenced by multiple sources, including river input, terrestrial transport, settling of suspended sediment, and wind-wave action. Thus, when applying grain-size EMs analysis, it is necessary to have a thorough understanding of the potential sources and identify the possible EM types and characteristics (Dietze et al., 2012).

Second, the sample collection and analysis needs to be considered. To obtain reliable results, representative sampling points should be selected within the tidal flat area, and the sample collection and processing procedures should follow strict protocols to avoid potential contamination and sample distortion. For grain-size analysis, laser grain-sizers or sieving methods can be used.

Third, in terms of EM identification and interpretation, interpretation of the grain-size data is required to determine the possible EM types and relate them to the sediment sources in the tidal flat. This involves integrating geological background knowledge, geomorphological features, and source characteristics (Dietze and Dietze, 2019).

Fourth, in terms of statistical analysis and validation, statistical methods need to be employed to validate the results of grain-size

EMs analysis. For example, Q-mode cluster analysis, principal component analysis, and other methods can be used to evaluate the similarities and differences between the different samples. Additionally, comparing the results with other indicators, such as the geochemical parameters and isotopic compositions, can further validate the findings of the grain-size EMs analysis.

The grain-size EMs analysis method also has certain limitations (Dietze et al., 2022). The quantified sediment source that is obtained through grain-size EM calculations can reflect the sediment source structure in the study area. However, in terms of the variations in the structure of the different sources, it may not necessarily represent the actual changes in the sources. Therefore, the potential causes of the source variations should be analyzed considering the coastal evolution, natural conditions, and human activities in the study area. In particular, vegetation succession and coastal engineering activities can lead to changes in the sediment characteristics without changes in the sediment sources. Due to the complexity and diversity of the sources and the influence of sedimentation processes and resuspension, there may be uncertainties in the results of grain-size EMs analysis. Therefore, when applying the grain-size EMs analysis method, it is necessary to consider other geological, geomorphological, and geochemical evidence to obtain a more comprehensive and reliable interpretation of the sediment sources.

5 Conclusion

This study used the grain-size EM analysis method to identify and quantify sediment cores from typical areas of the muddy coastal tidal flats in the central part of Jiangsu Province, namely Dongtai on the south side and Sheyang on the north side. The results were as follows:

(1) Both Sheyang and Dongtai were primarily composed of sand and silt, with a lower clay content. The average grain size of Sheyang and Dongtai varied significantly with depth, showing a decreasing trend and reduced grain size fluctuations with decreasing depth. This change was particularly evident at 56 cm in Sheyang and 60 cm in Dongtai.

(2) The average grain size of each EM in the sediment cores from Sheyang and Dongtai increased over time, while the clay content gradually decreased, and the content of silt and sand increased. The grain-size distribution curves of each EM exhibited an unimodal near-normal distribution. EMs 1-3 in Sheyang were derived from the abandoned Yellow River, EM 4 was derived from the Yangtze River and the NJRSR, and EM 5 was derived from the NJRSR. EMs 1-4 in Dongtai all originated from the abandoned Yellow River, EM 5 originated from the Yangtze River, and EM 6 originated from the Yangtze River and the NJRSR.

(3) On a century scale, the sediment in Sheyang was composed of 73.91% from the abandoned Yellow River source and 26.09% from the Yangtze River and NJRSR sources. The sediment in Dongtai consisted of 70.55% from the abandoned Yellow River source and 29.45% from the Yangtze River and NJRSR sources. The average sediment contribution from the abandoned Yellow River and the Yangtze River and NJRSR to the mud-coast tidal flats in the central part of Jiangsu Province was 72.23% and 27.77%, respectively. Over time, the contribution of the abandoned Yellow River to the sediment in the mud-coast tidal flats showed an increasing trend. On a spatial scale, the contribution of the abandoned Yellow River decreased from north to south in the coastal tidal flats. The sediment characteristics and sources of the mud-coast tidal flats were influenced by factors such as the spread of *Spartina alterniflora*, sediment transport from the Yangtze River, and complex coastal hydrodynamic conditions. Due to similar grain-size characteristics and complex sedimentary environments, it was difficult to distinguish the sediments from the Yangtze River and the NJRSR using the grain-size EM analysis method.

(4) The grain-size EM analysis method can effectively avoid the influence of grain-size effects and has shown good potential for source analysis of sediment cores. However, due to the complexity and diversity of the sources and the influence of sedimentation and resuspension processes, when applying the grain-size EM analysis method, other geological, geomorphological, and geochemical evidence should be considered in light of the coastal evolution, natural conditions, and human activities in the study area to obtain a more comprehensive and reliable interpretation of the sediment sources.

Data availability statement

The raw data supporting the conclusions of this article will be made available by the authors, without undue reservation.

Author contributions

YL: Formal analysis, Investigation, Methodology, Writing – original draft, Writing – review & editing. YZ: Writing – review & editing. WX: Formal analysis, Supervision, Writing – review & editing. NL: Investigation, Methodology, Writing – review & editing. MX: Conceptualization, Funding acquisition, Project administration, Supervision, Writing – review & editing.

Funding

The author(s) declare financial support was received for the research, authorship, and/or publication of this article. This work was supported by the Marine science and technology innovation project of Jiangsu province (No. JSZRHYKJ202103), National Natural Science Foundation of China (No. 41801005), Natural Science Foundation of Jiangsu Province (No. BK20200735) and the Postgraduate Research & Practice Innovation Program of Jiangsu Province (No. KYCX23_1726).

Conflict of interest

The authors declare that the research was conducted in the absence of any commercial or financial relationships that could be construed as a potential conflict of interest.

The author(s) declared that they were an editorial board member of Frontiers, at the time of submission. This had no impact on the peer review process and the final decision.

Publisher's note

All claims expressed in this article are solely those of the authors and do not necessarily represent those of their affiliated organizations, or those of the publisher, the editors and the reviewers. Any product that may be evaluated in this article, or claim that may be made by its manufacturer, is not guaranteed or endorsed by the publisher.

References

Barbier, E. B., Hacker, S. D., Kennedy, C., Koch, E. W., Stier, A. C., and Silliman, B. R. (2011). The value of estuarine and coastal ecosystem services. *Ecol. Monographs.* 81, 169–193. doi: 10.1890/10-1510.1

Cao, J., Zhao, Y., Xu, M., Liu, Q., and Shi, W. (2021). Quantitative geochemistry as a provenance indicator for surface sediments in the north Jiangsu radial sand ridges (NJRSR) in the South Yellow Sea, East China. *Continental Shelf Res.* 228, 104545. doi: 10.1016/j.csr.2021.104545

De Winter, R. C., and Ruessink, B. G. (2017). Sensitivity analysis of climate change impacts on dune erosion: case study for the Dutch Holland coast. *Climatic Change.* 141, 685–701. doi: 10.1007/s10584-017-1922-3

Dietze, E., and Dietze, M. (2019). Grain-size distribution unmixing using the R package EMMAgeo. *E&G Quaternary Sci. J.* 68, 29–46. doi: 10.5194/egqsj-68-29-2019

Dietze, E., Hartmann, K., Diekmann, B., Ijmker, J., Lehmkuhl, F., Opitz, S., et al. (2012). An end-member algorithm for deciphering modern detrital processes from lake sediments of Lake Donggi Cona, NE Tibetan Plateau, China. *Sedimentary Geology.* 243, 243–244. doi: 10.1016/j.sedgeo.2011.09.014

Dietze, M., Schulte, P., and Dietze, E. (2022). Application of end-member modelling to grain-size data: Constraints and limitations. *Sedimentology.* 69, 845–863. doi: 10.1111/sed.12929

Dou, Y., Yang, S., Liu, Z., Shi, X., Li, J., Yu, H., et al. (2012). Sr-Nd isotopic constraints on terrigenous sediment provenances and Kuroshio Current variability in the Okinawa Trough during the late Quaternary. *Palaeogeogr. Palaeoclimatol. Palaeoecology.* 365, 38–47. doi: 10.1016/j.palaeo.2012.09.003

Folk, R. L. (1971). Longitudinal dunes of the northwestern edge of the Simpson Desert, Northern Territory, Australia, 1. Geomorphology and grain size relationships. *Sedimentology.* 16, 5–54. doi: 10.1111/j.1365-3091.1971.tb00217.x

Fu, M., and Zhu, D. (1986). The sediment sources of the offshore submarine sand ridge field of the coast of Jiangsu Province. *J. Nanjing University(Natural Science).*, 536–544.

Gao, W. (2015). *Sediment dispersal processes on the southern Yellow Sea continental shelf: tracer methods* (Nanjing, China: Nanjing University).

Gao, S., Collins, M. B., Lanckneus, J., Moor, G. D., and Lancker, V. V. (1994). Grain size trends associated with net sediment transport patterns: An example from the Belgian continental shelf. *Mar. Geology.* 121, 171–185. doi: 10.1016/0025-3227(94)90029-9

Gao, J., Jia, J., Kettner, A. J., Xing, F., Wang, Y., Li, J., et al. (2018). Reservoir-induced changes to fluvial fluxes and their downstream impacts on sedimentary processes: The Changjiang (Yangtze) River, China. *Quaternary Int.* 493, 187–197. doi: 10.1016/j.quaint.2015.03.015

Gao, J., Shi, Y., Sheng, H., Kettner, A. J., Yang, Y., Jia, J., et al. (2019). Rapid response of the Changjiang (Yangtze) River and East China Sea source-to-sink conveying system to human induced catchment perturbations. *Mar. Geology.* 414, 1–17. doi: 10.1016/j.margeo.2019.05.003

Gao, S., Wang, D., Yang, Y., Zhou, L., Zhao, Y., Gao, W., et al. (2016). Holocene sedimentary systems on a broad continental shelf with abundant river input: process-product relationships. *Geological Society London Special Publications.* 429, 223–259. doi: 10.1144/SP429.4

Li, Y., and Gao, S. (2012). Heavy metal characteristics in the sediment cores from the Changjiang subaqueous delta. *Mar. Sci. Bull.* 31, 154–161. doi: 10.3969/j.issn.1001-6392.2012.02.005

Li, M., Wu, S., Gong, X., Yang, L., Gou, F., and Li, J. (2022). Characteristics of coastline change under the influence of human activities in central Jiangsu Province from 1989 to 2019. *Mar. Sci.* 46, 60–68. doi: 10.11759/hykx/20210512003

Li, S., Yang, S., Liang, M., Cheng, T., Chen, H., and Liu, N. (2018). The end member model analysis on grain size of loess in the eastern tibetan plateau. *Earth Environment.* 46, 331–338. doi: 10.14050/j.cnki.1672-9250.2018.46.107

Li, C., Zhang, Y., Yuan, S., Shao, L., Jiang, H., Zhou, Y., et al. (2010). Grain size characteristics and origin of the "Wushan loess"at wushan area. *Earth Science.* 35, 879–884. doi: 10.3799/dqkx.2010.102

Li, C., and Zhao, J. (1995). Recent research and controversy of the Jianggang radial sand ridge in northern Jiangsu Province. *Mar. Sci.*, 57–60.

Liu, S., Gao, J., Xu, X., Shi, Y., Shu, Z., Wu, H., et al. (2021). Response of sediment grain size composition of the Zhe-Min coastal mud to the sediment load reduction of the Changjiang River entering the sea. *Haiyang Xuebao.* 43, 105–115. doi: 10.12284/hyxb2021025

Lu, H., and An, Z. (1998). Paleoclimatic significance of particle size distribution of loess in the Loess Plateau, China. *Scientia Sinica(Terrae).* 28, 6. doi: 10.1007/BF02878745

Meng, K. (2018). *Study on modern sedimentary characteristics and spatial-temporal distribution of heavy metals in nearshore tidal flats of radiating sand ridges in northern Jiangsu Province.* (Nanjing, China: Nanjing Normal University).

Murray, N. J., Clemens, R. S., Phinn, S. R., Possingham, H. P., and Fuller, R. A. (2014). Tracking the rapid loss of tidal wetlands in the Yellow Sea. *Front. Ecol. Environment.* 12, 267–272. doi: 10.1890/130260

Paterson, G. A., and Heslop, D. (2015). New methods for unmixing sediment grain size data. *Geochemistry.* 16, 4494–4506. doi: 10.1002/2015GC006070

Purkait, B. (2010). The use of grain-size distribution patterns to elucidate aeolian processes on a transverse dune of Thar Desert, India. *Earth Surface Processes Landforms.* 35, 525–530. doi: 10.1002/esp.1939

Rao, W., Mao, C., Wang, Y., Su, J., Balsam, W., and Ji, J. (2015). Geochemical constraints on the provenance of surface sediments of radial sand ridges off the Jiangsu coastal zone, East China. *Mar. Geology.* 359, 35–49. doi: 10.1016/j.margeo.2014.11.007

Sahu, B. K. (1964). Depositional mechanisms from the size analysis of clastic sediments. *J. Of Sedimentary Res.* 34, 73–83. doi: 10.1306/74D70FCE-2B21-11D7-8648000102C1865D

Sun, Y., Gao, S., and Li, J. (2003). Preliminary analysis of environmentally sensitive grain-size components in land-derived sediments of marginal seas. *Chin. Sci. Bulletin.* 48, 83. doi: 10.1360/03tb9038

Sun, Q., Zhou, J., and Xiao, J. (2001). Grain-size characteristics of Lake Daihai sediments and its paleaoenvironment significance. *Mar. Geology Quaternary Geology.* 21, 93–95. doi: 10.16562/j.cnki.0256-1492.2001.01.016

Visher, G. S. (1969). Grain size distributions and depositional processes. *J. Of Sedimentary Res.* 39, 1074–1106. doi: 10.1306/74D71D9D-2B21-11D7-8648000102C1865D

Wang, Y., Wen, Y., Wang, J., and Zhang, R. (2006). Feasible rate of tidal flat reclamation—Jiangsu mud coast as a case study. *Mar. Sci. Bulletin.* 25, 15–20. doi: 10.3969/j.issn.1001-6392.2006.02.003

Wang, Z., Yu, D., Wang, W., Luo, F., Tang, J., and Yang, J. (2021). End-member analysis of sedimentary dynamics lndicated by the grain-size of surface sediments in the quanzhou bay. *Trop. Geography.* 41, 975–986. doi: 10.13284/j.cnki.rddl.003377

Weltje, G. J. (1997). End-member modeling of compositional data: Numerical-statistical algorithms for solving the explicit mixing problem. *Math. Geology.* 29, 503–549. doi: 10.1007/BF02775085

Xu, M., Meng, K., Zhao, Y., and Zhao, L. (2019). Sedimentary environment evolution in east China's coastal tidal flats: the north Jiangsu radial sand ridges. *J. Coast. Res.* 35, 524–533. doi: 10.2112/JCOASTRES-D-18-00006.1

Xu, W., Peng, X., Jia, P., and Wang, M. (2014). Spatial-temporal coastline evolution of the old Yellow River delta, northern Jiangsu Province. *J. Nanjing University(Natural Sciences).* 50, 576–584. doi: 10.13232/j.cnki.jnju.2014.05.005

Xu, Y., Zou, X., and Zuo, P. (2009). The effect of the alien species to the coastal ocean environment–take *spartina alterniflora* for example. *Henan Science.* 27, 609–612. doi: 10.3969/j.issn.1004-3918.2009.05.028

Xue, C., Jia, J., Gao, S., Cai, T., Chao, H., Li, J., et al. (2018). The contribution of middle and small rivers to the distal mud of subaqueous Changjiang Delta: results from Jiaojiang River and Oujiang River. *Haiyang Xuebao.* 40, 75–89. doi: 10.3969/j.issn.0253-4193.2018.05.007

Yang, Y. (2017). *Late Quaternary sediment provenance and environment evolution on the central Jiangsu coast* (Nanjing, China: Nanjing University).

Yang, S., Wang, Z., Guo, Y., Li, C., and Cai, J. (2009). Heavy mineral compositions of the Changjiang (Yangtze River) sediments and their provenance-tracing implication. *J. Asian Earth Sci.* 35, 56–65. doi: 10.1016/j.jseaes.2008.12.002

Yu, Q., Wang, Y., Shi, B., Wang, Y., and Gao, S. (2017). Physical and sedimentary processes on the tidal flat of central Jiangsu Coast, China: Headland induced tidal eddies and benthic fluid mud layers. *Continental Shelf Res.* 133, 26–36. doi: 10.1016/j.csr.2016.12.015

Zhang, Y. (1990). A study of characteristics and sources of clay minerals of sediments in coastal areas of Jiangsu province. *Mar. Science.* 2, 34–42.

Zhang, W., Ma, H., Ye, L., Dong, C., Yu, L., and Feng, H. (2012). Magnetic and geochemical evidence of Yellow and Yangtze River influence on tidal flat deposits in northern Jiangsu Plain, China. *Mar. Geology.* 319, 47–56. doi: 10.1016/j.margeo.2012.07.002

Zhang, X., Wang, W., Yan, C., Yan, W., Dai, Y., Xu, P., et al. (2014). Historical coastline spatio-temporal evolution analysis in Jiangsu coastal area during the past 1000 years. *Scientia Geographica Sinica.* 34, 344–351.

Zhang, X., Zhai, S., and Xu, S. (2006). The application of grain-size end-me mber modeling to the shelf near the estuary of Changjiang River in China. *Haiyang Xuebao.* 28, 159–166. doi: 10.3321/j.issn:0253-4193.2006.04.021

Zhao, Y., Liu, Q., Huang, R., Pan, H., and Xu, M. (2020b). Recent evolution of coastal tidal flats and the impacts of intensified human activities in the modern radial sand ridges, east China. *Int. J. Environ. Res. Public Health* 17, 3191. doi: 10.3390/ijerph17093191

Zhao, C., Qin, C., and Teng, J. (2020a). Mapping large-area tidal flats without the dependence on tidal elevations: A case study of Southern China. *ISPRS J. photogrammetry Remote sensing.* 159, 256–270. doi: 10.1016/j.isprsjprs.2019.11.022

Zhao, Y., Xu, M., Liu, Q., Shu, Q., and Wang, P. (2021). Centennial scale environmental changes in the elemental geochemistry of tidal flat sediments in the northern Jiangsu radial sand ridges. *Haiyang Xuebao.* 43, 66–80.

Zhu, H., Zhang, Y., and Li, C. (2020). The application of end-member analysis in ldentification of paleo-floods in wuhan section of the yangtze river. *Acta Sedimentologica Sinica.* 38, 297–305. doi: 10.14027/j.issn.1000-0550.2019.039